

# AN EXPERIMENTAL STUDY ON THE EFFECT OF RESTRICTED ORIFICE SURGE TANK

By Sukeyuki SHIMA\*, C.E. Member and Mikio HINO\*\*, C.E. Accos. Member

**Synopsis :** Experiments on water-hammer phenomena have been carried out. Comparisons between theoretical and observed water-hammer waves are shown. The effect of restricted orifice surge tank for the case of rapid closure of gate has especially been studied, and also comparisons between theory and experiments are shown, which demonstrate a considerably fair agreement. Adialogram for estimating the effect of the restricted orifice surge tank is presented.

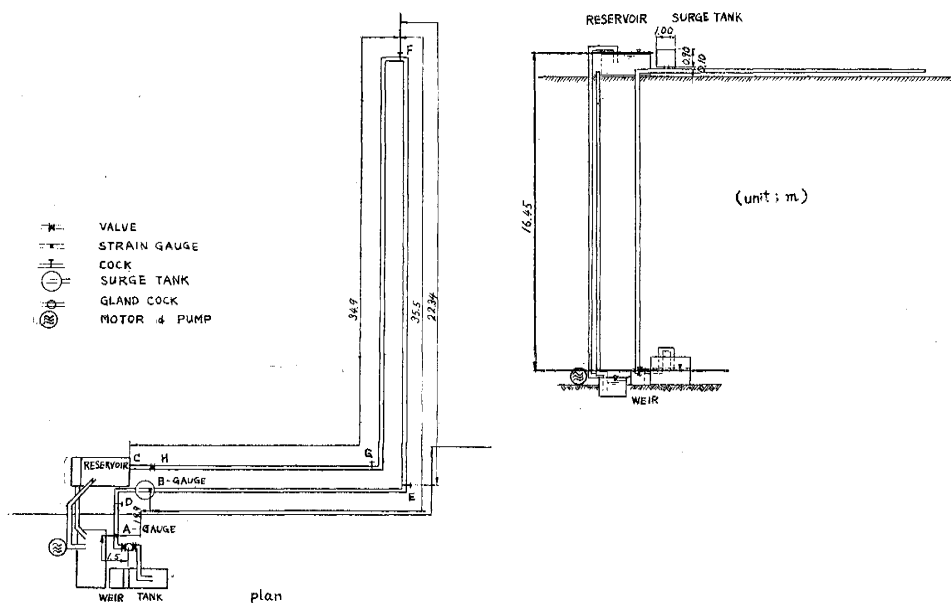
## INTRODUCTION

The surge tank installed in the system of a reservoir, pressure tunnel and penstock has two objects, i.e., one to reflect the high water-hammer pressure and prevent it from being transmitted to the upstream pressure tunnel, demanding a large port area, and the other to absorb and damp out the surging mass energy between reservoir and surge tank, demanding a large energy loss. These objects are opposed to each other. To fulfill these demands, several types of surge tank, such as differential and restricted-orifice types, have been proposed. This study treats only with the restricted orifice type, especially the transmission coefficient for the case of rapid closure of gate.

## EXPERIMENTAL EQUIPMENTS AND PROCEDURES

(a) **Model of the system** General arrangements are shown in Fig 1. A reservoir, a pipe line made of steel (10.5 cm inside diameter and 0.5 cm in wall thickness), a surge tank (100 cm diameter), a gate (gland cock), a low tank, and a measuring weir constitute a circulation system. The circulating water was pumped up to the reservoir by the 10 HP pump, and the excess water pumped up to the reservoir was overflowed directly to the low tank through another pipe. Total pipe length was 91.8 m and total head obtained was 16.45 m. The surge tank was installed at a distance of 21.1 m from the gate, and several sizes of orifice were inserted at the base of the tank. The section of the tank was made large

Fig. 1 General arrangements



\* Assistant Professor, University of Tokyo, M.J.S.C.E.

\*\*Graduate School, Civil Engineering, University of Tokyo, A.M.J.S.C.E.

enough to avoid the effect of surging head. The observed surface rise due to surging was only several centimeters, and this may be negligible compared to the total head amounting to 16.45 m. Cocks (D, E, F, and G of Figure 1) were installed to let out the entrapped air in the pipe, cocks E and F were also used as clinging holes for a pressure gauge to measure wave velocity and for a manometer to calibrate the strain gauges. Valve H was used to close up the water in pipe tight and to introduce high pressure by jack at the time of gauge calibration.

(b) **Recording apparatus** Water-hammer pressures produced by rapid closure of the gland cock (gate) were received by strain gauges attached to the pipe at points A and B. Variations in voltage in the Wheatstone bridge circuit, the resistance components of which the strain gauges compose were amplified by DM-type strain meter (a product of KYOWA MUSEN, CO., Japan) and recorded by an oscillograph.

(c) **Wave velocity measurement** To calculate water-hammer pressure, the wave velocity of water-hammer must be determined. The theoretical expression of wave velocity is generally given by

$$\alpha = \sqrt{\frac{1}{W \left( \frac{1}{K} + \frac{D}{bE} \right)}} \dots \dots \dots (1)$$

where

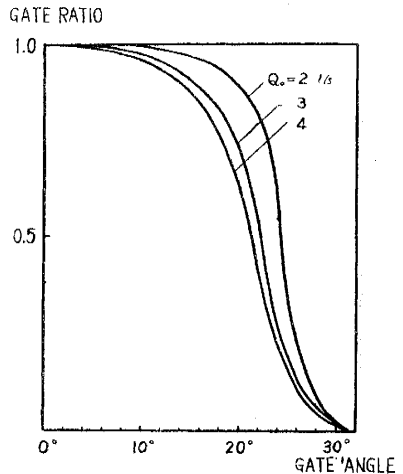
- W = specific weight of water
- K = bulk modulus of compression of water
- E = modulus of elasticity of conduit material
- D = diameter of conduit
- b = thickness of pipe wall

In many cases, however, the actual wave velocity decreases below this theoretical value due probably to entrained air bubbles or air masses entrapped in pipe. In fact, our measurements showed the variation of this value in the range of 1400-1100 m/sec, while the theoretical value is about 1400 m/sec according to Equation (1).

Therefore, the wave velocity was determined from frequency of water-hammer wave oscillation between the gate and reservoir, or from the time necessary for water-hammer wave to travel from points A to F. In the latter case, the pressure gauge was also installed at point F.

(d) **Characteristics of gate** To solve the water-hammer wave theoretically, the characteristics of gate (gland cock in this experiment), i.e., the orifice law coefficient, is indispensable as a boundary condition at the tail end of the pipe line. To obtain this characteristic curve of the gate, the relation between the opening angle of the cock and the discharge rate were measured in a steady state, although the phenomena may occur in transient state. The characteristics vary greatly depending on the initial discharge rate as shown in Fig. 2. The opening angle of gate was recorded simultaneously with water-hammer wave on the oscillograph papers.

Fig. 2 Characteristics of gate



(e) **Head loss** The total head loss was of the order of several centimeters. This may be negligible compared to the total head.

(f) **Orifice diameter** In this study eleven diameters of orifices were used, as shown in Table 1. The area of the conduit is denoted by \$A\_0\$, and that of each orifice by \$A\_p\$.

Table 1 Orifice diameters used in the experiments

No. of orifice	0	1	2	3	4	5	6	7	8	9	10	11
diameter (cm)	0	0.10	0.38	0.69	1.07	1.21	1.68	2.27	2.96	3.79	4.40	5.57
\$A_p/A_0\$	0	\$9.07 \cdot 10^{-5}\$	\$1.31 \cdot 10^{-3}\$	\$4.32 \cdot 10^{-3}\$	\$1.03 \cdot 10^{-2}\$	\$1.33 \cdot 10^{-2}\$	\$2.54 \cdot 10^{-2}\$	\$4.65 \cdot 10^{-2}\$	\$7.92 \cdot 10^{-2}\$	\$1.30 \cdot 10^{-1}\$	\$1.76 \cdot 10^{-1}\$	\$2.81 \cdot 10^{-1}\$

**COMPARISON BETWEEN EXPERIMENTAL AND THEORETICAL CURVES**

The solution of the water-hammer equations is not so easy to obtain theoretically, since, while they represent the forms of the typical wave equation, the boundary condition at the gate is non-linear. Several methods are available today including the most useful "graphical or characteristic-line method" proposed by BDRGERON<sup>1)</sup> and ANGUS<sup>2)</sup>.

To check the degree of agreement between theory and experiment, experiments were conducted for the simple pipe line system with the closed orifice of the surge tank. Here only two examples of comparison are presented, which show fair agreement between theory and experiment. (see **Figs. 3 and 4**)

**Fig. 3 Comparison between theoretical and observed water-hammer wave**

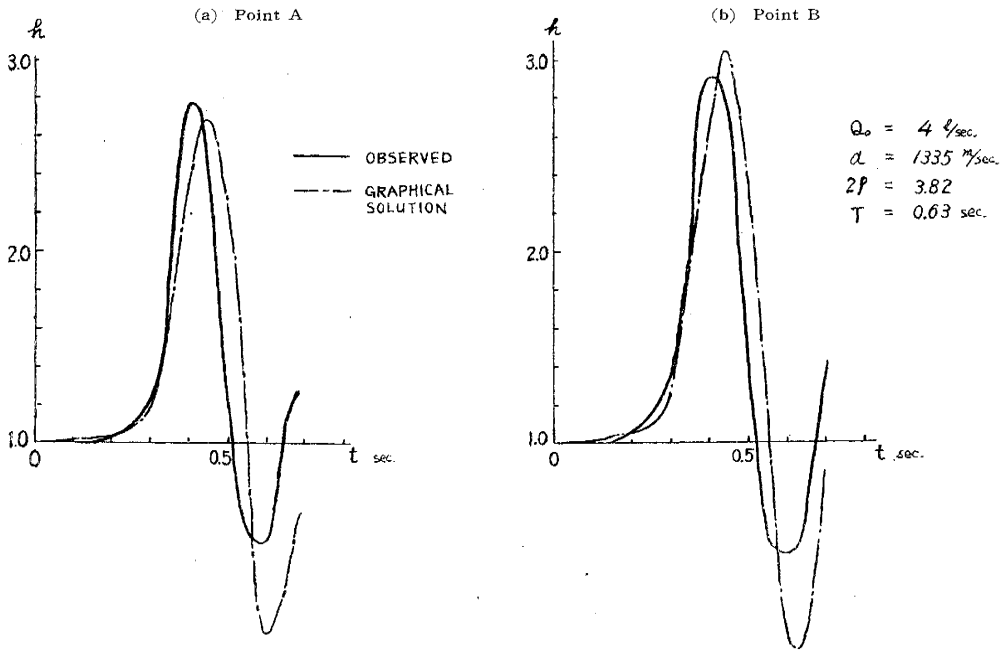
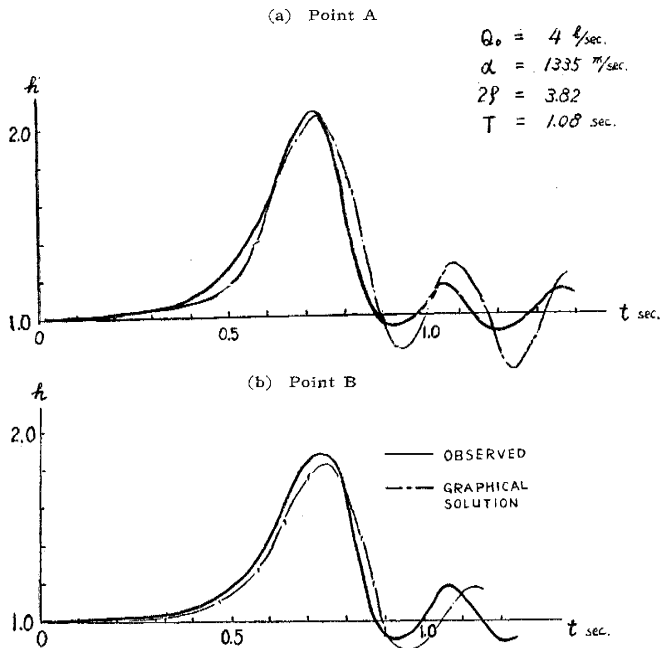


**Fig. 4 Comparison between theoretical and observed water-hammer wave**



The observed oscillograph records do not agree with the theoretical results when the pressures drop below those of the steady state conditions. This may be attributed to the rapid drop of pressure below the atmospheric pressure, resulting in separation of the dissolved air from the water, and also in irregular reflection of wave and decrease in wave velocities.

**TRANSMISSION COEFFICIENT FOR THE CASE OF INSTANTANEOUS CLOSURE OF GATE**

(a) **Theory** The equations of motion and continuity applied to a unit length of pipe yield the following fundamental equations of water-hammer waves<sup>3)</sup>,

$$\alpha^2 \frac{\partial^2 H}{\partial x^2} = \frac{\partial^2 H}{\partial t^2}, \dots\dots\dots(2)$$

$$\alpha^2 \frac{\partial^2 V}{\partial x^2} = \frac{\partial^2 V}{\partial t^2}, \dots\dots\dots(3)$$

Where  $H$ =total head (water-hammer plus steady state)  
 $V$ =flow velocity  
 $\alpha$ =wave velocity as defined in Eq. (1)  
 $x$ =distance from the tail end (gate) of pipe  
 $t$ =time

These are the typical wave equations, and the general solutions are given as follows,

$$H - H_0 = F\left(t - \frac{x}{\alpha}\right) + f\left(t + \frac{x}{\alpha}\right) \dots\dots\dots(4)$$

$$V_0 - V = \frac{g}{\alpha} F\left(t - \frac{x}{\alpha}\right) + \frac{g}{\alpha} f\left(t + \frac{x}{\alpha}\right) \dots\dots\dots(5)$$

Considering  $H$  and  $V$  at points A and B at the time  $t_A$  and  $t_B$ , respectively, where  $t_B - t_A = (x_B - x_A)/\alpha$ , the relation between  $H_A$ ,  $H_B$ ,  $V_A$  and  $V_B$  can be expressed from Equations (4) and (5) using nondimensional form,

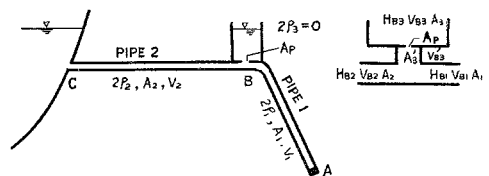
$$h_B - h_A = \pm 2 \rho (v_B - v_A) \dots\dots\dots(6)$$

where  $h = H/H_{A0}$ ,  $v = V/V_{A0}$ ,  $2 \rho = \alpha V_{A0}/gH_{A0}$ .

This is the so-called characteristic line equation. The suffix o denotes the initial conditions, the positive sign in Eq. (6) the progressing waves propagating opposite to the initial flow direction, and the negative sign the reflected waves.

A system of restricted orifice surge tank such as shown in Figure 5 was treated neglecting the water-hammer phenomena in the surge tank. The suffixes 1, 2 and 3 apply to penstock, pressure tunnel and surge tank, respectively (Fig. 5).

**Fig. 5 Restricted-orifice surge tank system**



Now let us consider the rapid closure of gate. The gate closes perfectly before the reflected wave

front, initiated at the gate and reflected at the orifice entrance, reaches the gate, or before the initial wave front reaches the reservoir. At this moment of perfect closure  $h_A$  becomes equal to  $2 \rho_1 + 1$  or  $\alpha_1 V_{A0}/gH_{A0} + 1$ , propagating upstream. It is represented by the characteristic line equation,

$$h_{B1} - h_A = 2 \rho_1 (v_{B1} - v_A) \dots\dots\dots(7)$$

where  $h_A = 2 \rho_1 + 1$ ,  
 $v_A = 0$

Also for pipe 2, we obtain,

$$h_{B2} - h_C = -2 \rho_2 (v_{B2} - v_C), \dots\dots\dots(8)$$

where

$$h_C = 1 \text{ and } u_C = 1.$$

And at the junction,

$$\text{(continuity eq.) } u_{B2} = u_{B1} + u_{B3}' \dots\dots\dots(9)$$

$$\begin{aligned} \text{(equal head condition)} \quad h_{B_1} &= h_{B_2} = h_{B_3} + av_{B_3}'^2 \dots\dots\dots (10) \\ h_{B_3} &= 1, \end{aligned}$$

where  $a$  is a non-dimensional head loss coefficient at the orifice.

Only the friction loss of restricted orifice is considered, neglecting the loss due to the bending of pipe. Solving these equations the following relations are obtained,

$$v_{B_3}' = \{-\rho_{12} + \sqrt{\rho_{12}^2 + 4\rho_{12}a}\}/a \dots\dots\dots (11)$$

$$h_{B_1} = \{1 - \sqrt{1 + 4a/\rho_{12}}\}^2 / \frac{a}{\rho_{12}^2} \dots\dots\dots (12)$$

etc.

The transmission coefficient is defined by

$$\begin{aligned} \lambda &= (h_{B_1} - h_{A_0}) / (h_A - h_{A_0}), \\ &= (h_{B_1} - 1) / (h_A - 1) \dots\dots\dots (13) \end{aligned}$$

Therefore, using Eq. (12) this is rewritten

$$\lambda = \left\{ 1 - \sqrt{1 + \frac{4a}{\rho_{12}}} \right\}^2 / \frac{2a\rho_{12}}{\rho_{12}^2} \dots\dots\dots (14)$$

where

$$2\rho_{12} = \alpha_1 V_{A_0} / gH_{A_0},$$

$$2\rho_{12} = \left( \frac{\alpha_1 \alpha_2}{\alpha_1 + \alpha_2} \right) V_{A_0} / gH_{A_0},$$

$$a = \xi \cdot \rho_1 \cdot (A_1/A_3')^2 \cdot V_{A_0} / \alpha_1 = \xi / 2 gH_{A_0} \cdot (A_1 V_{A_0} / A_3')^2,$$

$\xi$  = head loss coefficient of orifice defined by

$$\Delta H = \xi \cdot V_{B_3}'^2 / 2g.$$

In our experiments,  $2\rho_{12} = 2\rho_2 = 2\rho$ ,  $2\rho_{12} = \rho$ , and  $A_1 = A_2 = A_3 = A_0$ . Therefore, Eq. (14) is simplified further,

$$\lambda = \left\{ 1 - \sqrt{1 + \left( \frac{8a}{\rho} \right)} \right\}^2 / \left( \frac{8a}{\rho} \right) \right\} \dots\dots\dots (15)$$

$$a/\rho = \xi V_{A_0} / \alpha_1$$

The head loss coefficient  $\xi$  is expressed as

$$\xi = (A_0/A_P - 1)^2 \dots\dots\dots (16)$$

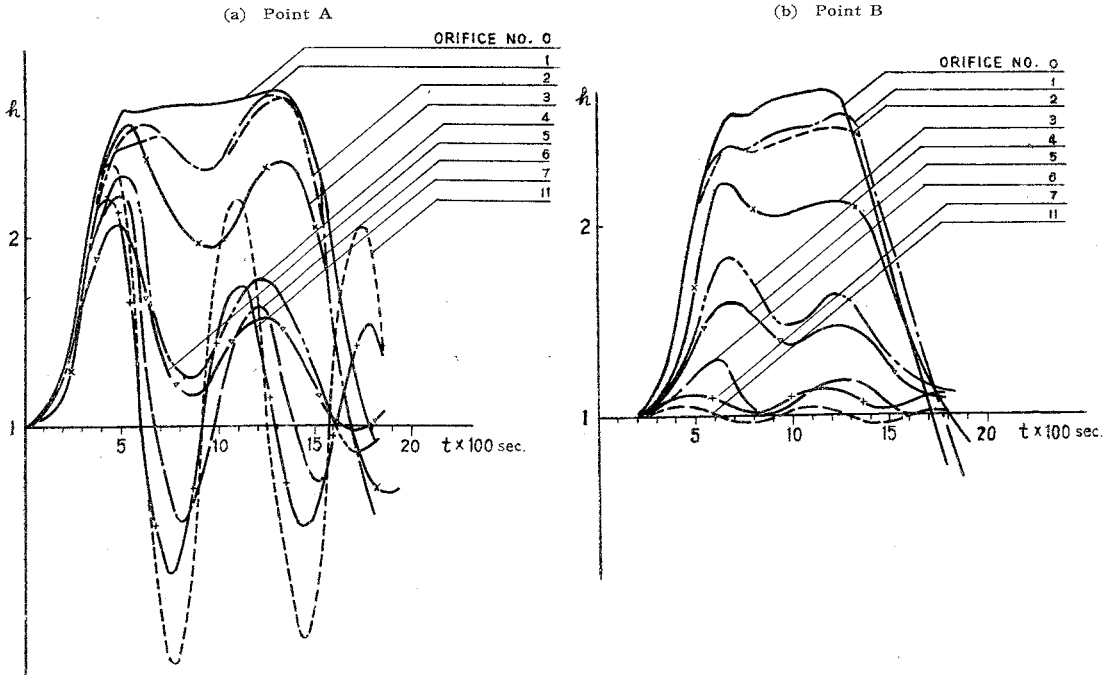
(b) **Results of experiments** Before discussing the transmission coefficients, the general behaviors of water-hammer waves due to the effect of different sizes of orifice diameter will be stated. In **Fig. 6**, which plots on the same graph a representative oscillograph record from each size of orifice, excepting Nos. 8, 9, and 10 to avoid confusion, the gradual wave deformations at Points A and B due to the reflection of negative waves at the tank are shown. By closing the gate rapidly, the excessive high pressure is produced at the gate converting the kinetic energy of the flowing water to the elastic work of stretching the conduit wall and compressing the water. The pressure propagates upstream and is partially reflected at the surge tank as a negative wave. The rapid drop of the water-hammer pressures at about 0.05 sec represents this stage. Further, this negative wave is reflected also as a negative wave at the gate and travels upstream, and is reflected again this time as a positive wave. This corresponds to the rapid increase in pressures at about 0.14 sec. In the meanwhile large negative pressures arise, which have been initially produced at the gate, transmitted through the junction of conduits at the tank toward the reservoir and then reflected there as large negative pressures.

In accordance with the increasing orifice area, the effect of the surgetank becomes remarkable. For the orifice area 13.0% of that of the conduit, denoted No. 9, the surge tank may be considered to act already as a reservoir capable of transmitting the negligible water-hammer pressure only.

The experiments were carried out at the uniform discharge rate of 2 liter/sec.

In our experiments, the closure time ranged from 0.03 to 0.05 sec. But, considering the gentle slopes of the characteristic curves for the beginning and last stages of gate closure (see **Fig. 2**), the effective closure time in our experiments will be regarded as sufficiently rapid. In fact, it has been noticed that the observed transmission coefficients were independent from the closure time of gate within the ranges

Fig. 6 Water-hammer wave deformation



stated above. Strictly speaking, however, it is advisable to limit the rapid closure time within about 0.03 sec ( $\approx 2 AB/\alpha_1$ ).

The transmission coefficients were obtained as the ratios of the maximum pressure increase at point B to the corresponding maximum pressure increase at point A for each run of the experiments.

In Fig. 7, the experimental results are compared with the theoretical curve calculated from exs. (15) and (16). Each plot is an average of three or four experimental values, the errors ranging within  $\pm 3\%$ . Two different symbols stand for the different dates of the experiments. The scatter of the plots may be attributed to a slight change in pipe conditions, i.e., the entrapped air bubbles and masses which play most important role in the actual behaviors of water hammer. As the orifice area is increased, the effect of the mechanical vibration of the conduit becomes significant, since it is superimposed on the oscillograph records of the water-hammer pressure.

Fig. 7 shows a considerable agreement between theory and experiments. The transmission coefficients of the restricted-orifice surge tank are increased when the orifice area is reduced below 10% of the conduit area.

Fig. 7 The transmission coefficient experimental and theoretical.

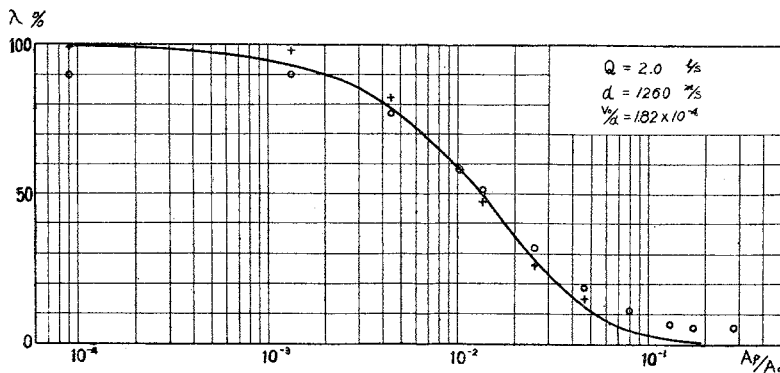


Fig. 8 shows a group of the transmission coefficient curves calculated from eqs. (15) and (16) for the case of rapid closure of gate for each parameter  $V_0/\alpha$ .

Fig. 8 A parametric family of curves for the transmission coefficient in the restricted orifice surge tank.

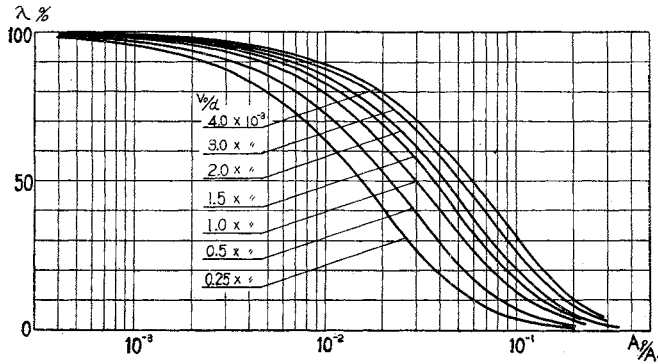


Fig. 9 gives an example from the graphical solution<sup>4)</sup> of the water-hammer wave for the case of the gradual closure of gate, where the reflected negative wave from the reservoir has not reached.

CONCLUSIONS

The results of the experiments show that the effect of the restricted-orifice surge tank changes rapidly as the orifice area is reduced below a certain percentage of the conduit area which is dependent on the ratio of the initial flow velocity to the velocity of wave (see Fig. 8).

The wave deformation due to the different transmission coefficients of the tank are visualized in the same graph, which may serve to understand the role of the restricted-orifice surge tank.

ACKNOWLEDGEMENTS

The research was initiated by the suggestion of Professor Masashi Hom-ma, University of Tokyo, Japan. The authors wish to express their hearty thanks to Yusuke HIROSAWA, research assistant, who rendered valuable assistance in experiments and preparing diagrams; also to Messrs. Haruto HATA, Sumio ODA, Keiichi TANAKA and Mitsuhiro YAMAGUCHI, then students of civil engineering at University of Tokyo, who participated in the experiments.

Fig. 9(a) Comparison between calculated and observed water-hammer wave in the pipe-line system with a restricted-orifice surge tank.

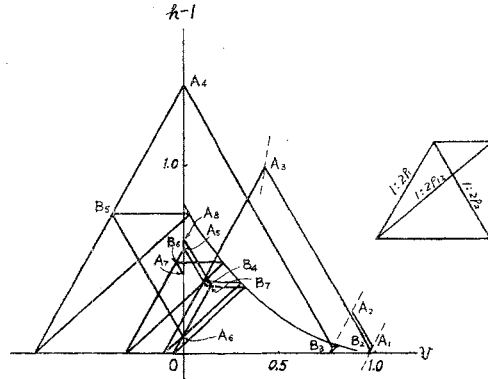
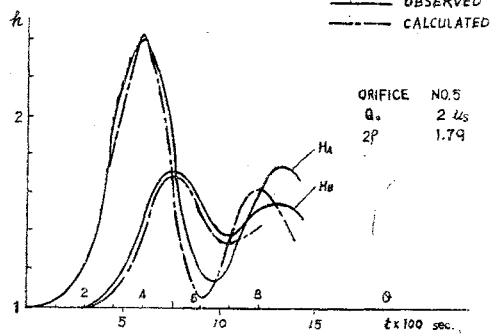


Fig. 9(b) Graphical solution procedure.



BIBLIOGRAPHY

- 1) BERGERON, L.: Etude des variations de regime dans les conduits d'eau, Revue General de l'Hydraulique, vol.1, Nos. 1 et 2, (1935)
- 2) ANGUS, R.W.: Water-hammer pressures in compound and branched pipes, Trans. ASCE, Vol. 104, (1939).
- 3) Rich, G.R.: Hydraulic Transients, McGraw-Hill, New York (1951).
- 4) Benini, G.: Sui fenomeni di colpo d'ariete nelle gallerie munite di pozzo piezometrico con luce strozzata, L'Energia Elettrica, Vol. 27 (1950).